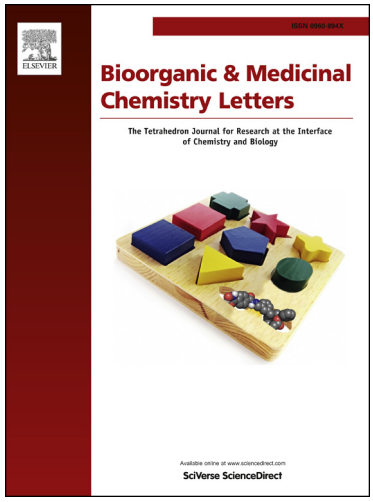

Discovery and optimization of a highly efficacious class of 5-aryl-2-aminopyridines as FMS-like tyrosine kinase 3 (FLT3) inhibitors

Gang Liu, Sunny Abraham, Xing Liu, Shimin Xu, Allison M. Rooks, Ron Nepomuceno, Alan Dao, Daniel Brigham, Dana Gitnick, Darren E. Insko, Michael F. Gardner, Patrick P. Zarrinkar, Ron Christopher, Barbara Belli, Robert C. Armstrong, Mark W. Holladay

PII: S0960-894X(15)00727-1
DOI: http://dx.doi.org/10.1016/j.bmcl.2015.07.023
Reference: BMCL 22912

To appear in: *Bioorganic & Medicinal Chemistry Letters*

Received Date: 29 June 2015
Revised Date: 8 July 2015
Accepted Date: 9 July 2015

Please cite this article as: Liu, G., Abraham, S., Liu, X., Xu, S., Rooks, A.M., Nepomuceno, R., Dao, A., Brigham, D., Gitnick, D., Insko, D.E., Gardner, M.F., Zarrinkar, P.P., Christopher, R., Belli, B., Armstrong, R.C., Holladay, M.W., Discovery and optimization of a highly efficacious class of 5-aryl-2-aminopyridines as FMS-like tyrosine kinase 3 (FLT3) inhibitors, *Bioorganic & Medicinal Chemistry Letters* (2015), doi: http://dx.doi.org/10.1016/j.bmcl.2015.07.023

Graphical Abstract

To create your abstract, type over the instructions in the template box below.
Fonts or abstract dimensions should not be changed or altered.

Discovery and optimization of a highly efficacious class of 5-aryl-2-aminopyridines as FMS-like tyrosine kinase 3 (FLT3) inhibitors

Leave this area blank for abstract info.

Gang Liu* Sunny Abraham, Xing Liu, Shimin Xu, Allison M. Rooks, Ron Nepomuceno, Alan Dao, Daniel Brigham, Dana Gitnick, Darren E. Insko, Michael F. Gardner, Patrick P. Zarrinkar, Ron Christopher, Barbara Belli, Robert C. Armstrong, Mark W. Holladay

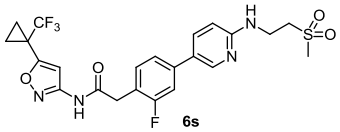

6s

MV4-11 IC_{50} = 0.2~0.3 nM
highly efficacious at 1 mg/kg/d p.o.

Bioorganic & Medicinal Chemistry Letters
journal homepage: www.elsevier.com

Discovery and optimization of a highly efficacious class of 5-aryl-2-aminopyridines as FMS-like tyrosine kinase 3 (FLT3) inhibitors

Gang Liu[a,*] Sunny Abraham[a], Xing Liu[a], Shimin Xu[a], Allison M. Rooks,[b] Ron Nepomuceno,[b] Alan Dao,[b] Daniel Brigham,[b] Dana Gitnick,[c] Darren E. Insko,[c] Michael F. Gardner,[c] Patrick P. Zarrinkar,[d] Ron Christopher,[c] Barbara Belli,[b] Robert C. Armstrong,[b] Mark W. Holladay[a]

[a]*Departments of Medicinal Chemistry,* [b]*Cell Biology and Pharmacology,* [c]*DMPK and Toxicology,* [d]*Technology Development, Ambit Biosciences Corporation, 11080 Roselle St., San Diego, CA 92121, U.S.A.*

ARTICLE INFO

Article history:
Received
Revised
Accepted
Available online

Keywords:
Feline McDonough sarcoma (FMS)-like tyrosine kinase 3 (FLT3); aminopyridine; hinge binding motif; CYP3A4; time-dependent inhibition

ABSTRACT

Based on a putative binding mode of quizartinib (AC220, **1**), a potent FMS-like tyrosine kinase 3 (FLT3) inhibitor in Phase III clinical development, we have designed de novo a simpler aminopyridine-based hinge binding motif. Further optimization focusing on maximizing in vivo efficacy and minimizing CYP3A4 time-dependent inhibition resulted in a highly efficacious compound (**6s**) in tumor xenograft model for further preclinical development.

* Corresponding author. Tel.: +1-224-622-2484; e-mail: liugx1@gmail.com

Feline McDonough sarcoma (FMS)-like tyrosine kinase 3 (FLT3) is a membrane-bound receptor tyrosine kinase (RTK) expressed by immature hematopoietic cells. When activated by its ligand (FLT3L), FLT3 supports the proliferation and survival of hematopoietic progenitors, and is important for the normal development of stem cells and the immune system.[1] Acute myeloid leukemia (AML) develops as the consequence of a series of genetic changes in hematopoietic precursor cells. Approximately one third of AML patients harbor an internal tandem duplication (ITD) in the juxtamembrane domain of FLT3. The FLT3/ITD mutation leads to a constitutive, ligand-independent activation of the tyrosine kinase function, and is known to confer a poor prognosis in patient survival.[2] Therefore, FLT3 has emerged as an attractive drug target to improve outcomes for AML patients with the ITD mutation. Over the past decade, several TK inhibitors targeting FLT3 have been studied in clinical settings to treat AML, but have met with limited success.[3] More recently, quizartinib (AC220, **1**), discovered from this laboratory,[4] has emerged as a more potent and selective FLT3 inhibitor with significant clinical activity, including high bone marrow response rates in relapsed and refractory FLT3/ITD AML patients.[5]

In contemplating the characteristics that might constitute a good back up compound to **1**, the superior in vivo efficacy of **1** along with a better safety profile were determined to be highly desirable. In search of a novel starting point for the project, compound **1** was examined as a possible inspiration for de novo design given its excellent overall profile. Since extensive SAR has been conducted around the existing pharmacophore, it was decided that a more radical alteration of the structure might be beneficial. We did not have the benefit of the actual binding mode of **1** to FLT3 determined using X-ray crystallography until long after this project concluded;[6] molecular modeling work was published soon after the conclusion of the project.[7] For the purpose of de-constructing the structure of **1**, we assumed that **1** would bind to FLT3 in a similar fashion as sorafenib (another known FLT3 inhibitor) binds to BRAF kinase.[8] Such assumption would put the benzo[d]imidazo[2,1-b]thiazole ring of **1** in the region for interacting with the hinge of the FLT3 kinase (Scheme 1). We set out to re-engineer the hinge binder of **1** to create smaller, simpler motifs that will interact potently with the target protein, with a particular focus on monocyclic amino heteroaryl moieties to provide the requisite H-bond donor-acceptor arrays.

Since the ethoxymorpholinyl tail of **1** mainly serves the purpose of enhancing solubility of **1**,[4b] the newly designed hinge binders lacked such extra motif. As shown in Table 1, among the newly designed six-membered heteroaryls, amino group para to the central phenyl ring connection appeared to be preferred over the meta-position (**3a** vs. **3b**). All of the 4-aminoheteroaryl-based analogs (**3b, 3d-e**) with the exception of pyridazine derivative (**3c**) bound to FLT3 kinase domain with sub-nanomolar affinity,[9] and exerted potent inhibition of the proliferation of MV4-11 cells, a FLT3 dependent human leukemia cell line harboring a homozygous FLT3-ITD mutation. Aminothiazole derivative (**3f**), a 5-membered aminopyridine bioisostere, fared somewhat worse in cells, and aminoimidazole analogue (**3g**) was much less active.

The amino heteroaryls were also found to possess reasonable selectivity for the kinome based on a comprehensive screening panel profiling, as measured by the S(10) score.[10] Since most of these analogs had low liver microsomal turnover (>50% remaining after 60 min incubation), screening rat PK was installed in the early part of the flow scheme for triaging compounds. Compound **3d** exhibited a promising rat PK profile:[11] moderate clearance (18.7 mL/min/kg), good exposure after oral dosing at 10 mg/kg (AUC of 41.7 μM·h), and excellent oral bioavailability (163%). We assumed for the time being that the >100% bioavailability represented saturation of a clearance mechanism in the oral arm of the study. Overall, the 2-aminopyridine-5-aryl analogue **3d** exhibited very similar in vitro/PK profile to **1**, and was selected as the main scaffold for lead optimization.

Scheme 1. De novo design of monocyclic aminoheteroaryl-based hinge binding motifs

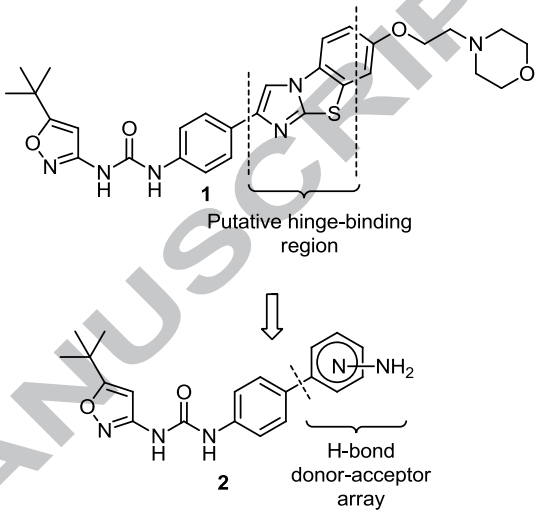

Table 1. Amino heteroaryls as the new hinge binding motifs

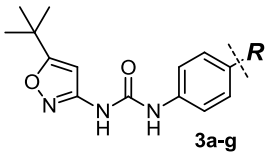

Compd	-***R***	FLT3 K_d[a] (nM)	Prolif. IC_{50}[a] (nM)	S(10) Score
1	NA	1.3	0.25	0.061
3a	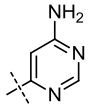	2.1	nd[c]	0.036
3b	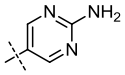	0.8	0.5	0.145
3c	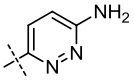	2.1	2.7	0.019
3d	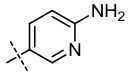	0.4	0.3	0.089
3e	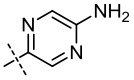	0.3	0.4	0.15
3f	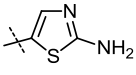	0.8	1.7	0.120
3g	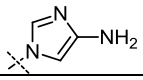	0.9	77.7	0.058

[a] Each experiment was run in duplicate and the values shown are the average of the two. [b] in MV4-11 cells. [c] nd: not determined.

In comparison to **1**, there was still room for improvement in the kinome specificity with the aminopyridine scaffold. As demonstrated by the X-ray crystal structure of sorafenib in complex with BRAF, only one of the urea N-Hs makes critical hydrogen-bond interaction with the αC-helix.[8] Therefore, we rationalized that removal of the proximal N-H to the central phenyl ring should be tolerated and can potentially offer opportunities for structural diversity. A number of alternatives to urea linkers were explored, including both carbon and nitrogen-based connections. As shown in Table 2, the analogue with a methylene linker (**4a**) matched the corresponding urea compound in terms of in vitro potency and cellular activity. The other modifications (**4b**-**e**) suffered significant loss of cellular activity. The rat PK profile of acetamide **4a** was also encouraging: moderate clearance (11 mL/min/kg), reasonable exposure after oral dosing at 10 mg/kg (AUC of 28 μM·h), and high oral bioavailability (65%). The biaryl acetamide was used as the preferred template for further SAR study to provide another layer of structural diversion from **1**.

Table 2. Modifications of the urea linker

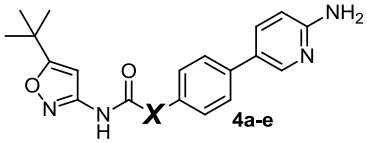

Compd	-*X*	FLT3 K_d [a] (nM)	Prolif. [b] IC_{50} [a] (nM)	S(10) Score
4a	CH_2	1.1	0.3	0.095
4b	-NMe	0.9	25.6	0.088
4c	CF_2	0.6	26.3	0.052
4d	CHOH	1.7	5.1	0.036
4e	$CHNH_2$	5.07	167	0.034

[a] Each experiment was run in duplicate and the values shown are the average of the two. [b] in MV4-11 cells.

The focus was then turned to the isoxazole portion of the molecule. Previously, we have learned that the *t*-butyl group of the isoxazole of **1** can be oxidized (i.e. hydroxylation) in vivo.[12] Based on the experience with another kinase inhibitor project,[13] a number of fluorinated variations of the *t*-butyl isoxazole were examined to mitigate the potential oxidation, hydroxylated *t*-butyl and cyclopropylmethyl modifications were also probed. A number of these modifications (**5a**, **5c**-**g**) were well tolerated whereas cell activity of the hydroxylated *t*-butyl derivative **5b** decreased substantially. Particularly, the trifluoromethylcyclopropane in place of the *t*-butyl group led to analogue **5c**, which retained the high cellular potency and selectivity. When compared to **4a**, the rat PK of **5c** did not show the expected lowering in clearance (10.4 mL/min/kg), yet the oral exposure (AUC of 33 μM·h) and oral bioavailability (83%) did increase modestly. The 3-aminoisoxazole of **3d** and **5c** can also be switched to the corresponding 5-aminoisoxazole (**5f**-**g**) without too much change in either cell activity or kinome selectivity.

Table 3. Modifications of the *t*-butyl isoxazole in **4a**.

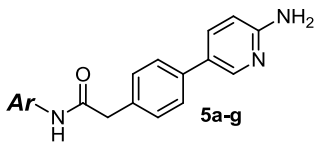

Compd	-Ar	FLT3 K_d [a] (nM)	Prolif. [b] IC_{50} [a] (nM)	S(10) Score
5a	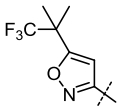	0.705	0.282	0.117
5b	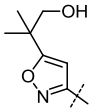	0.455	8.25	0.044
5c	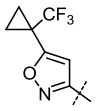	0.178	0.348	0.071
5d	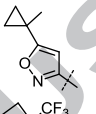	0.137	1.04	0.078
5e		0.485	0.3	0.119
5f		0.839	0.342	0.114
5g	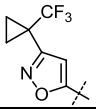	0.684	0.396	0.093

[a] Each experiment was run in duplicate and the values shown are the average of the two. [b] in MV4-11 cells.

During broad profiling of the lead structure, one particular aspect of deficiency for this series of compounds was identified. The prototype compounds, such as **4a** and **5c**, had undesirable inhibitory activity versus cytochrome P450 (CYP) isoform 3A4 with IC_{50} values in the low micromolar range (data not shown).[14] Suspecting that the electron-rich aminopyridine ring was the culprit in inducing strong interaction with the heme of the CYP enzyme, we introduced electron-withdrawing fluorine at various positions of the molecule. As shown in Table 4, CYP3A4 inhibition was rather sensitive to the position of the fluorination. Neither 3- (**6a**) nor 6-position (**6c**) fluorination of the pyridine ring provided any relief in CYP3A4 inhibition, while 4-F on the aminopyridine ring led to compound **6b** with a clean CYP3A4 profile. Fluorination of the central phenyl ring also had divergent effect on CYP3A4 inhibition, with 2-fluoro-substitution (**6d**) substantially reducing CYP3A4 inhibition and 3-fluorophenyl ring (**6e**) still retaining significant CYP3A4 activity.

Encouraged by this early success, a substantially more stringent hurdle was put in place to select compounds with best possible profiles. Time-dependent inhibition of CYP3A4 often indicates generation of reactive metabolite(s), and can have implications in potential drug-drug interactions.[15] When **6d** was incubated with human liver microsomal protein in the presence of NADPH for 30 minutes prior to the initiation of CYP assay, the IC_{50} value against CYP3A4 dropped to 2.2 μM. For the purpose of triaging compounds, a threshold of 10 μM IC_{50} value in CYP3A4 inhibition with 30 min pre-incubation was established.

In addition to installing electron-withdrawing groups directly on the aminopyridine/central phenyl rings, another area for

mitigating CYP3A4 inhibition was the amino group of the pyridine ring. Substitution off the amino group may hinder the interaction with CYP enzyme by virtue of steric hindrance, while electron-withdrawing groups would be expected to further reduce the propensity to interact with the heme iron center. We have examined several simple substitutents (e.g. Me and Et) off the amino group, and found minimal impact on the in vitro/cellular properties (data not shown), which made this position a potentially productive area for modulating the drug-like properties of resulting analogues without compromising potency.

The more elaborate amino substituents we focused on were alkylsulfonylethyl groups, which combined both the electron-withdrawing and metabolic stability properties offered by the sulfone group. To our delight, both the methanesulfone (**6f**) and ethanesulfone (**6g**) analogues retained excellent in vitro activities, in addition to a clean CYP3A4 profile (IC_{50} > 10 μM with or without pre-incubation). The SAR of the alkylsulfonylethyl groups was then expanded to confirm the broader utility of such groups.

Interestingly, the combination of 3-F and methanesulfonylethyl group (**6h**) resulted in substantial loss of cell activity. Both the secondary and tertiary sulfonamide analogues (**6l-m**) were potent in cells with good kinome selectivity. Unfortunately, they suffered from poor oral bioavailability in rats (9% and 7%, respectively). Both the cyclopropylsulfonylethyl (**6n**) and the extended methanesulfonylpropyl (**6o**) derivatives worked well. For the non-sulfone analogues, the N,N-diethylacetamide compound **6p** was slightly less potent in the MV4-11 cell proliferation assay. The reverse sulfonamide also produced a potent analogue (**6g**), albeit with poor rat bioavailability (2%). Interestingly, a tertiary amyl alcohol group could mimic the methanesulfonylethyl group, providing compound **6r** with a balanced profile of potent cell activity and clean CYP3A4. Combining the best sulfones off the amino group with the 2-F substituent in the central phenyl ring yielded a crop of highly potent compounds with minimal CYP inhibition in the time-dependent assay. Select examples (**6s-u**) are shown in Table 4.

Several lead compounds (**6f**, **6r-t**) were selected for a broader profiling of selectivity and ADMET properties (Table 5). In the selectivity cell assays versus other members of the PDGFR family kinases, all four compounds were shown to have 10-20 fold reduced potency in inhibiting the phosphorylation of Kit and PDGFRβ, in comparison o the corresponding pFLT3 IC_{50} values. These compounds were much more selective over CSF1R in the phosphorylation assay, demonstrating over 100-fold separation. These compounds were also clean in a patch clamp hERG channel inhibition assay with IC_{50} values greater than 10 μM. Even though these compounds were highly bound to plasma proteins, their high exposure in mouse after oral dosing in conjunction with potent cellular activity predicted sufficient target coverage with once daily dosing.

The antitumor efficacy of compounds **6f** and **6r-t** was assessed at 1 mg/kg orally once daily (QD), an efficacious dose for compound **1** in a subcutaneous flank-tumor xenograft model in athymic nude mice using the MV4-11cell line. With respect to tumor growth delay (TGD) and Log cell kill at equivalent dose, all of these compounds with the exception of **6f** exceeded the performance of **1** (TGD = 44 d and log cell kill = 2.0) (Table 5).[16] Additional factors, including tissue distribution and enzyme binding kinetics, might have affected the performance of the compounds in the xenograft model, in addition to cell activity and plasma exposures.

Compound **6s** appeared to have the most robust response in delaying the progression of tumor at the 1 mg/kg dose. It was further evaluated in a dose response study in the same MV4-11 xenograft model with doses of 0.1, 1, and 10 mg/kg for 2 weeks (Figure 1). Compound **1**, used as a positive control, was dosed at 0.1 and 10 mg/kg. As shown in Figure 1, **6s** potently inhibited the progression of tumor in a dose-dependent fashion, even at an extremely low dose of 0.1 mpk. At the higher doses, tumors regressed completely and long-lasting tumor growth suppression persisted for an extended period after dosing was halted. Minimal body weight loss (<5%) was observed in animals treated with **6s** at all doses, indicating that it was well tolerated in mice at the efficacious doses. As a biomarker of FLT3 inhibition, the pFLT3 level in the tumors was also measured in a separate acute study. Dose-dependent inhibition of FLT3 phosphorylation with **6s** (up to 79% inhibition of pFLT3 versus vehicle control at 10 mpk dose) was found to be consistent with tumor growth inhibition occurring via inhibition of the FLT3 signaling pathway.

The synthesis of urea analogues mostly originated from an initial Suzuki coupling between boronic acid **7** and heteroaryl bromides **8**, followed by acid-mediated removal of the N-Boc protecting group to give the biaryl intermediate **9** (Scheme 2). The more reactive anilino amine group of **9** reacted with the known carbamate **10** to generate urea analogues **2**.[17]

Figure 1. In vivo efficacy and pFLT3 inhibition of compound **6s** in mouse xenograft model.

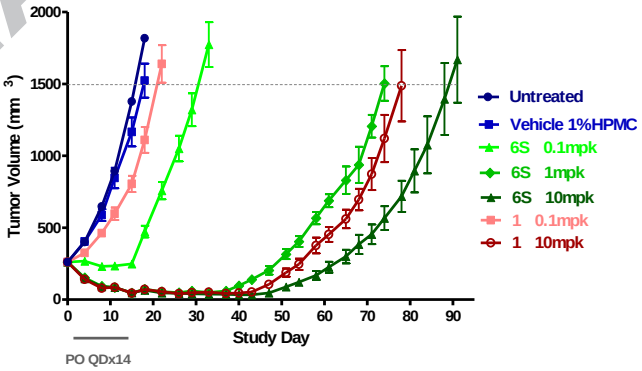

The phenylacetamides were prepared according to the sequence outlined in Scheme 3. Acylation of the anion of acetonitrile with various esters **11** yielded ketonitriles **12**, which were cyclized with hydroxylamine using a two-step procedure to provide 3-aminoisoxazoles **13**. On the other hand, bromophenylacetic acids **14** were converted to the corresponding boronate esters **15** via a Suzuki-Mukiyama coupling. Condensation of **13** with **15** afforded the key intermediates **16**. The aminopyridines **18** were prepared from nucleophilic substitution of 2-fluoropyridines **17** with various amines. A second Suzuki-Mukiyama coupling between **16** and **18** gave the phenylacetamides **19**.

Scheme 2.[a] General synthetic routes to urea analogues.

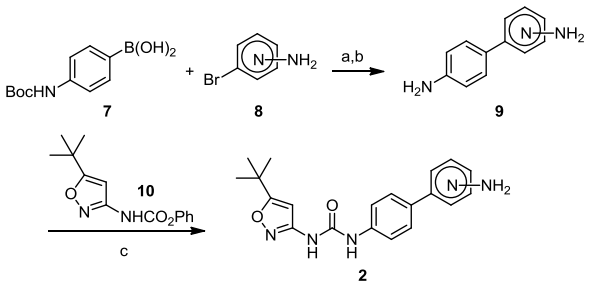

[a] Reagents and conditions : (a) $Pd(PPh_3)_4$, Na_2CO_3, water, 1,4-dioxane, 170 °C, 20 min, 97%; (b) TFA, DCM, rt, 4h, 70%; (c) DMAP, DMF, 50 °C, 16h, 71%.

Scheme 3.[a] General synthetic routes to phenylacetamide analogues.

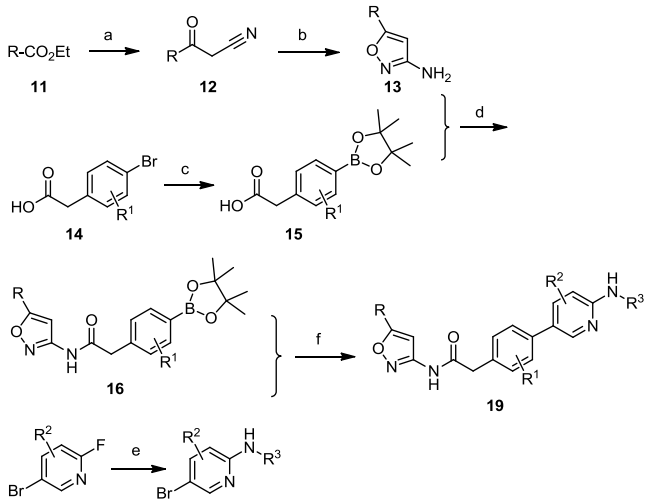

[a] Reagents and conditions: (a) NaH, CH_3CN, THF, 75 °C, 15 h, 29−93%; (b) $H_2NOH{\cdot}H_2SO_4$, NaOH (pH~8), MeOH/H_2O, 80 °C; then conc. HCl (pH~1), 80 °C, 4-6 h, 26−71%; (c) Bis(pinacolato)diborane, $PdCl_2$(dppf)·DCM, KOAC, DMF, 90 °C, 16 h, 90%; (d) HATU, DIEA, DMF, rt, 16 h, 25-54%; (e) H_2NR^3, DIEA, DMSO, 180 °C, 2h, 34-50%; (f) $PdCl_2$(dppf)·DCM, 2M aq. Na_2CO_3, CH_3CN, 90 °C, 1h, 30-80%.

In summary, our hypothesis on the putative binding mode of quizartinib (**1**) offered an opportunity to design de novo potent, monocyclic aminoheteroaryl-based FLT3 inhibitors. A systematic survey of the functionality around the aminopyridine ring led to analogues with improved CYP3A4 profile, including minimal time-dependent inhibition. A number of compounds demonstrated excellent in vivo efficacy in a tumor model of FLT3 ITD mediated proliferation. Based on the overall superior in vivo efficacy and drug-like properties, compound **6s** was selected for exploratory toxicology studies.

Table 4. SAR of 5-aryl-2-aminopyridine analogs

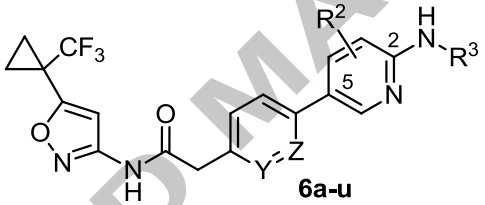

6a-u

Compd	Y	Z	R^2	R^3	FLT3 K_d[a] (nM)	Prolif.[b] IC_{50}[a] (nM)	pFLT3[b] IC_{50} (nM)	CYP3A4 IC_{50} (μM) without pre-incubation	CYP3A4 IC_{50} (μM) with 30 min incubation	S(10) Score
6a	CH	CH	3-F	H	0.68	0.128	0.2	3.5	1.4	0.101
6b	CH	CH	4-F	H	0.29	0.55	0.30	>40	nd[c]	0.142
6c	CH	CH	6-F	H	0.29	0.393	0.2	3.8	nd	0.07
6d	CF	CH	H	H	0.485	0.22	0.242	18.7	2.2	0.106
6e	CH	CF	H	H	0.351	0.959	0.25	1.8	nd	0.08
6f	CH	CH	H	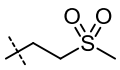	0.389	0.789	0.381	>40	17.9	0.034
6g	CH	CH	H	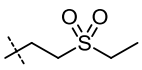	0.509	0.669	0.336	>40	>10	0.039
6h	CH	CH	3-F	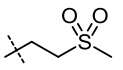	1.43	17.7	4.51	nd	nd	0.028
6l	CH	CH	H	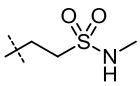	0.423	0.771	0.617	nd	>10	0.044
6m	CH	CH	H	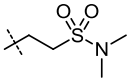	0.381	0.363	0.314	>40	nd	0.028
6n	CH	CH	H	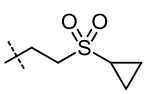	0.508	1	0.488	nd	19.5	0.029

6o	CH	CH	H	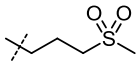	0.515	0.571	0.73	>40	>10	0.034
6p	CH	CH	H	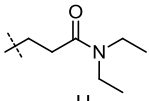	0.297	1.9	1.0	nd	nd	0.054
6q	CH	CH	H	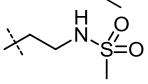	0.44	0.807	0.448	38	>10	0.023
6r	CH	CH	H	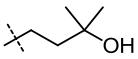	0.525	0.643	0.665	>40	10.5	0.073
6s	CF	CH	H	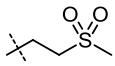	0.583	0.232	0.271	36.8	>10	0.093
6t	CF	CH	H	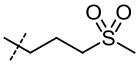	0.779	0.249	0.354	>40	16.8	0.054
6u	CF	CH	H	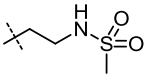	0.813	0.384	0.456	nd	9.5	0.039

[a] Each experiment was run in duplicate and the values shown are the average of the two. [b] in MV4-11 cells. [c] nd: not determined.

Table 5. Broader Profiles of Lead Compounds **6f**, **6r-t**

						Rat PK			Efficacy[f]	
AC Number Compd	pKit[a] IC_{50} (nM)	pCSF1R[b] IC_{50} (nM)	pPDGFRβ[c] IC_{50} (nM)	hERG[d] IC_{50} (μM)	Mouse/ human PPB (% unbound)	AUC p.o. (μM·h)	F (%) p.o.	Mouse PK[e] AUC (μM·h)	TGD (d)	Log Cell Kill
6f	18.2	216	18.5	>10	0.98/0.7	27.72	28	212	36	1.7
6r	7.14	85.7	34.2	>10	1.0/0.8	53.22	114.78	18	46	2.3
6s	4.48	221	15.7	>10	0.74/0.6	84.29	67	70	57	2.9
6t	6.01	159	22.4	>10	0.37/0.5	20.34	30.79	23	51	2.1

[c] in H526 cells. [b] in HEK293cells . [c] in MG-63 cells. [d] Patch clamp assay using CHO cells. [e] Female SCID mouse dosed orally at 10 mg/kg with 1% HMPC as vehicle. [f] Female SCID mouse implanted subcutaneously with MV4-11 were dosed at 1 mg/kg for 14 days.

Acknowledgments

We thank the KINOMEscan group at DiscoveRx for generating the binding K_ds and kinase specificity scores.

References and notes

1. Gilliland, D. G.; Griffin, J. D. *Blood* **2002**, *100*, 1532.
2. Sheikhha, M. H.; Awan, A.; Tobal, K.; Liu Yin, J. A. *Hematol. J.* **2003**, *4*, 41.
3. Kindler, T.; Lipka, D. B., Fischer, T. *Blood* **2010**, *116*, 5089.
4 (a) Zarrinkar, P. P.; Gunawardane, R. N.; Cramer, M. D.; Gardner, M. F.; Brigham, D.; Belli, B.; Karaman, M. W.; Pratz, K. W.; Pallares, G.; Chao, Q.; Sprankle, K. G.; Patel, H. K.; Levis, M.; Armstrong, R. C.; James, J.; Bhagwat, S. S. *Blood* **2009**, 114, 2984. (b) Chao, Q.; Sprankle, K. G.; Grotzfeld, R. M.; Lai, A. G.; Carter, T. A.; Velasco, A. M.; Gunawardane, R. N.; Cramer, M. D.; Gardner, M. F.; James, J.; Zarrinkar, P. P.; Patel, H. K.; Bhagwat, S. S. *J. Med. Chem.* **2009**, *52*, 7808.
5. Cortes, J. E.; Perl, A. E.; Dombret, H.; Dohner, H.; Steffen, B.; Rousselot, P. H.; Martinelli, G.; Estey, E.; Shah, N. P.; Burnett, A. K.; Gammon, G.; Trone, D.; Levis, M. J. *J. Clin. Oncol.* **2013**, 31, (suppl; abstr 7012).
6. Zorn, J. A.; Wang, Q,; Fujimura, E.; Barros, T.; Kuriyan, J. *PLoS ONE* **2015**, *10*, e0121177.
7. Smith, C. C.; Wang. Q.; Chin, C. S.; Salerno, S.; Damon, L. E.; Levis, M. J.; Perl, A. E.; Travers, K. J.; Wang, S.; Hunt, J. P.; Zarrinkar, P. P.; Schadt, E. E.; Kasarskis, A.; Kuriyan, J.; Shah, N. P. *Nature* **2012**, *485*, 260.
8. Wan, P. T. C.; Garnett, M. J.; Roe, S. M.; Lee, S.; Niculescu-Duvaz, D.; Good, V. M.; Cancer Genome Project; Jones, C. M.; Marshall, C. J.; Springer, C. J.; Barford, D.; Marais, R. *Cell* **2004**, *116*, 855.
9. The compounds described herein were tested for their binding affinity to the catalytic domain of FLT3 kinase in a competition binding assay with an ATP-competitive FLT3 inhibitor bound to a solid surface as described in the following reference: Fabian, M. A.; Biggs, W. H., III; Treiber, D. K.; Atteridge, C. E.; Azimioara, M. D.; Benedetti, M. G.; Carter, T. A.; Ciceri, P.; Edeen, P. T.; Floyd, M.; Ford, J. M; Galvin, M.; Gerlack, J. L.; Grotzfeld, R. M.; Herrgard, S.; Insko, D. E.; Insko, M. A.; Lai, A. G.; Lelias, J.-M.; Mehta, S. A.; Milanov, Z. V.; Velasco, A. M.; Wodicka, L. M.; Patel, H. K.; Zarrinkar, P. P.; Lockhart, D. J. *Nat. Biotechnol.* **2005**, *23*, 329.
10. Compounds were screened at 10 μM concentration against the KINOMEscan panel consisting of 386 individual wild-type kinases (mutants being excluded from this analysis). Selectivity score or S(10) is the ratio of kinase targets of the compound to the total number of kinases screened; kinases were defined as targets if the primary screen showed >90% competition (measured as < 10% of control experiment).
11. All the screening PK studies were done with Sprague Dawley rats, compounds were dosed at 1 and 10 mg/kg intravenously

(PEG400/water as vehicle) and orally (Pharmatek #6 as vehicle), respectively.

12. James, J.; Pratz, K.; Stine, A.; Apuy, J. L.; Insko, D. E.; Armstrong, R. C.; Zarrinkar, P. P.; Small, D.; Wierenga, W.; Levis. M. Presented at the American Society of Hematology 50th Annual Meeting, San Francisco, CA, December 2008; Poster #2637.
13. Rowbottom, M. W.; Faraoni. R.; Chao. Q.; Campbell, B. T.; Lai, A. G.; Setti, E.; Ezawa, M.; Sprankle, K. G.; Abraham, S.; Tran, L.; Struss, B.; Gibney, M.; Armstrong, R. C.; Gunawardane, R. N.; Nepomuceno, R. R.; Valenta, I.; Hua, H.; Gardner, M. F.; Cramer, M. D.; Gitnick, D.; Insko, D. E.; Apuy, J. L.; Jones-Bolin, S.; Ghose, A. K.; Herbertz, T.; Ator, M. A.; Dorsey, B. D.; Ruggeri, B.; Williams, M.; Bhagwat, S.; James, J.; Holladay, M. W. *J Med Chem*. **2012** *55*, 1082.
14 All the analogues examined exhibited no significant inhibition (i.e. IC_{50}s > 20 μM) versus four other CYP isoforms in the screening panel (1A2, 2C9, 2C19, 2D6).
15. Obach, R. S.; Walsky, R. L.; Venkatakrishnan, K. *Drug Metab. Dispos*. **2007**, *35*, 246.
16. Polin, L.; Corbett, T. H.; Roberts, B. J.; Lawson, A. J.; Leopold III, W. R.; White, K.; Kushner, J.; Hazeldine, S.; Moore, R.; Rake, J.; Horwitz, J. P. In *Tumor Models in Cancer Research*; Teicher, B. A., Ed.; Humana Press: New York, 2010; pp 43-78.
17. Gross, T. D.; Prasad, A. R.; Citineni, J. R. PCT patent applic. WO2011056939, **2011**.